Journal of Sol-Gel Science and Technology
https://doi.org/10.1007/s10971-024-06542-2

ORIGINAL PAPER

Sustainable synthesis of MFI zeolite and derived metal-acid bifunctional catalysts for hydroisomerization of *n*-heptane

Mengxuan Zhu[1] · Wenqi Xu[1] · Longyang Wang[1] · Rui Wang[1] · Heng Jiang[1] · Changzi Jin[1]

Received: 12 July 2024 / Accepted: 2 September 2024

Abstract

Developing sustainable synthesis method of versatile zeolites to overcome the shortcoming of traditional process is of significant for development of green chemistry and environmentally friendly techniques. In this work, MFI zeolite (ZSM-5) was synthesized through organotemplate-, solvent- and seed-free sustainable process comprising physical grinding and quasi-solid state crystallization and utilizing commercial silica gel or Stöber colloidal SiO_2 as silica source. The key influencing factors to this sustainable synthesis process, such as starting material composition, crystallization temperature and time, had been unambiguously investigated by combining a series of characterization techniques. It is revealed that the starting material with SiO_2/Al_2O_3 and Na_2O/SiO_2 at 30–40 and 0.072, respectively, is suitable to obtain zeolite product with high crystallinity. The presence of right amount of water (or alcohol) is also crucial. In addition, this green synthesis method can be extended into the fabrication of encapsulated metal-zeolite bifunctional catalyst, which is effective in hydroisomerization of *n*-heptane. These results are instructive for development of sustainable synthesis of aluminosilicate zeolites and derived heterogeneous catalysts.

Graphical Abstract

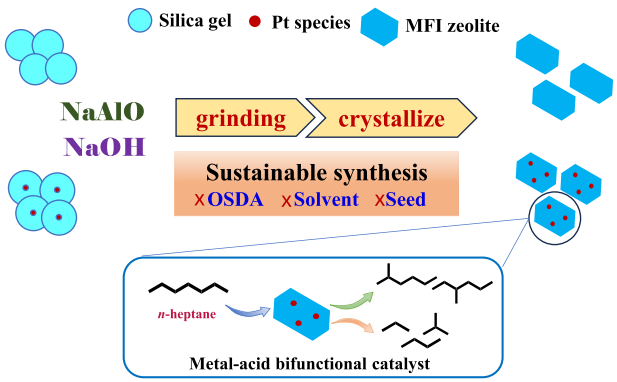

Keywords ZSM-5 zeolite · Sustainable synthesis · Bifunctional catalyst · Colloidal SiO_2 · Quasi-solid state transformation

Highlight

- SiO_2/Al_2O_3 of 30–40 and Na_2O/SiO_2 of 0.072 are crucial for sustainable synthesis of ZSM-5.
- The key role of water can be replaced by alcohol for successful synthesis of ZSM-5.
- The sustainable synthesis strategy is used to fabricate Pt-ZSM-5 bifunctional catalysts.
- The catalysts with encapsulation structure will be promising in hydroisomerization of n-heptane.

✉ Changzi Jin
jin_chz@163.com

[1] School of Petrochemical Engineering, Liaoning Petrochemical University, Fushun 113001, China

Published online: 07 September 2024

1 Introduction

Zeolites of crystalline aluminosilicate have attracted tremendous attentions for their prominent characters of large surface areas, uniform and abundant porosities, tunable acidity and excellent thermal/hydrothermal stability, which endow them wide application in the field of catalysis, adsorption and separation, ion exchange, energy transformation and so on [1–8]. Among those hundreds of reported zeolites, the MFI-type ZSM-5 zeolite is undoubtedly one of the most popular members because of its special three-dimensional channel system with 10-rings channel window, which can be used as catalysts and catalyst supports in oil refining, petrochemical and fine chemicals processing and exhibit outstanding performance [9–21]. Heavy use of zeolite materials has led to creased demand of reasonable zeolite preparation. However, the conventional preparation method of ZSM-5, as well as some other important zeolites, is hydrothermal process that consuming organic structural directing agents (OSDA) and plenty of water as solvent, usually existing the cost and environment problems [22–27]. For example, the consumption of expensive organic templates will result in high cost of synthesis process. Both the template and the decomposition products of template (NO_x, CO_2) are almost noxious. In addition, large amount of water in hydrothermal system not only produce lots of waste liquid, but the dissolution of Si- and Al-nutrients in solvent lead to the loss of zeolite product yield. Therefore, the development of sustainable economic and green synthesis routes without organic template and solvent for important zeolites is of significance and much-anticipated [28–33].

In general, the functions of templates in the zeolite synthesis involve structure-directing, channel-filling and charge-balance [34]. So, other alternatives with similar roles are necessary in OSDA-free zeolite synthesis system. Fortunately, the ZSM-5 zeolite can be synthesized by various templating routes. Except the most commonly used tetrapropyl ammonium templates (TPAOH and TPABr), other organic amines such as n-butylamine and ethanediamine, alcohols and alkali metal ions can also act as templates for successful preparation of ZSM-5 zeolite [25–27, 35–39]. To pursue the goal of OSDA-free synthesis, the utilization of alkali metal ions and alcohols are seemed to be more promising. The most typical is sodium ions, which can induce the synthesis of ZSM-5 in template-free hydrothermal system and the obtained products possessing open channel even without calcination treatment. But the drawback of low yield still exists for the use of large amount of water solvent in synthetic system [40–44].

Until Xiao and coworkers pronounced sustainable synthesis strategy for ZSM-5 and some other zeolites by conflating organotemplate-free and solvent-free routes, the green synthesis of zeolites had made further substantial progress [29, 45–49]. The solid raw materials are first mixed and ground well and then suffered crystallization treatment, the crystalline zeolite can be prepared. Because there is no use water solvent, the crystal water in raw materials plays a crucial role in formation of zeolite products. The raw materials of this green OSDA-free synthesis process can be expanded from conventional commercial reagent to natural mineral, such as kaolin and illite, which further reduce the synthesis cost [50–53]. However, the metal impurities in natural materials have significant effect on synthesis of zeolites, hampering the clarification of key synthetic conditions in synthesis process. In addition, it worth noting that most aforementioned green synthesis process are assisted by pre-synthesized target zeolites as seed. As Wu et al. had stated, same synthetic system will generate amorphous product without seed [47]. Therefore, it is obvious that the sustainable synthesis strategy for ZSM-5 zeolite can be further optimized.

Herein, a sustainable OSDA-, solvent- and seed-free synthesis for ZSM-5 with commercial silica gel or prepared Stöber-derived silica spheres as raw materials is researched. The influences of system composition and crystallization parameters on product are investigated to clarify the crucial synthetic conditions of this sustainable synthesis process. The synthesized ZSM-5 zeolites are characterized. In addition, this sustainable synthesis method can be applied to fabricate metal-zeolite bifunctional catalysts for hydroisomerization of linear alkane.

2 Experimental

2.1 Chemicals

Silica gel (specific surface area: 350–460 m^2/g, pore size: 8–12 nm, SiO_2: 99%.) was purchased from Qingdao Xinchanglai Silica Gel Ltd. Tetraethylorthosilicate (TEOS), polyvinylpyrrolidone (PVP K30, M.W. = 38,000) and dihydrogen hexachloroplatinate ($H_2PtCl_6{\cdot}6H_2O$) were purchased from Shanghai Aladdin Biochemical Technology Co. Sodium aluminate ($NaAlO_2$), aluminium sulphate ($Al_2(SO_4)_3{\cdot}18H_2O$), sodium hydroxide, sodium carbonate, ethanol, ammonium chloride and ammonia hydroxide ($NH_3{\cdot}H_2O$, 25–28 wt %) were purchased from Tianjin Damao Chemical Co. The distilled water was homemade. All the reagents were used without further purification.

2.2 Synthesis of Pt nanoparticles

The Pt nanoparticles was synthesized by alcohol reduction process [54]. Firstly, 85.7 mg PVP and 1.08 mL H_2PtCl_6

aqueous solution (38.6 mM) were dissolved in 45 mL ethanol and 5 mL water. Then, the synthetic mixture was refluxed at 80 °C under stirring for 2 h. Finally, the generated black Pt nanoparticles were collected by centrifugation and were redispersed in ethanol for further use.

2.3 Synthesis of SiO_2 spheres and Pt@SiO_2

The SiO_2 colloidal spheres were synthesized by a well-known Stöber method with slight modification. In typical, 70 mL ethanol, 15 mL water and 4 mL $NH_3{\cdot}H_2O$ were mixed together, followed by the addition of 3.5 g TEOS. After stirring constantly at room temperature for 24 h, the SiO_2 colloidal spheres were obtained by centrifugation and dried at 100 °C. The synthesis process of Pt@SiO_2 is similar to SiO_2 spheres except for the additional introduction of recommended amount of Pt nanoparticles (0.025 mmol) preceding the addition of TEOS.

2.4 Sustainable synthesis of ZSM-5 and derived catalysts

The synthesis of ZSM-5 zeolite was performed by reported solid-state conversion. In a typical run, 1.5 g of silica source (silica gel or Stöber SiO_2 sphere), 0.10 g of $NaAlO_2$, 0.09 g of NaOH and 0.90 g of water were mixed by grinding for 10 min. Then the mixture was transferred into 25 mL Teflon-lined autoclave and heated at 170 °C for 24 h and the crystalline product can be obtained. For the synthesis of Pt@ZSM-5 catalyst, Pt@SiO_2 was used as silica source and other conditions remained unchanged. The H-form zeolites were obtained by ion-exchange of as-synthesized Na-form products in 1 M NH_4Cl aqueous solution at 80 °C for 8 h, followed by calcination process (550 °C, 4 h). This ion-exchange process needs to be repeated once.

For comparison, supported Pt/ZSM-5 catalyst was prepared with H-form ZSM-5 from Stöber SiO_2 sphere as carrier via incipient-wetness impregnation method.

2.5 Characterization

Powder X-ray diffraction (XRD) pattern was recorded in a Bruck D8 Advance powder X-ray diffractometer using Cu Kα radiation in 2θ range of 4–50°. Scanning electronic microscopy (SEM) images were taken on SU8010 field-emission scanning electronic microscope operating at 5 kV. Transmission electronic microscopy (TEM) and high resolution transmission electronic microscopy (HRTEM) images were taken on a JEM-2100 electronic microscope with an accelerating voltage of 200 kV. Nitrogen physical adsorption/desorption isotherms were measured on Quantachrome Autosorb-IQ2-MP physical adsorption apparatus. The specific surface areas were calculated using the BET method. Ammonia temperature programmed desorption (NH_3-TPD) measurements were performed on Quantachrome TPD/TDR-Pulsar chemisorption analyzer in the range of 150–600 °C at a ramp rate of 20 °C min^{-1}. The SiO_2/Al_2O_3 ratio in the samples was calculated according to the analysis results on Bruker D8 Tiger X-ray fluorescence (XRF) spectrometer. The Pt content in metal-zeolite bifunctional catalysts were analyzed by inductively coupled plasma spectrometry (ICP) on Agilent ICP-OES 725 instrument. X-ray photoelectron spectroscopy (XPS) was measured on Thermo Fisher Scientific ESCALAB Xi+ spectrometer (Al Kα, hv = 1480 eV).

2.6 Catalytic tests

Catalytic performance of the prepared catalysts for hydroisomerization of *n*-heptane were operated on a fixed-bed stainless steel reactor at atmospheric pressure. Before reaction, the catalyst (0.5 g) was reduced by H_2 flow at 400 °C for 2 h, and then was cooled to reaction temperature. The *n*-heptane was fed into reactor with HPLC pump at a weight hourly space velocity (WHSV) of 2.0 h^{-1} and the H_2/*n*-heptane molar ratio was fixed at 10. The reaction products were detected on Techcomp GC7890 equipped with a TM-PONA capillary column (50 m × 0.2 mm × 0.5 μm) and FID detector.

3 Results and discussion

3.1 Sustainable synthesis for ZSM-5 zeolite

The absolute green synthesis for ZSM-5 zeolite without using organotemplate, solvent and zeolite seed is described in Fig. 1. The starting materials are mixed by grinding in the absence of adequate solvent and further crystallize into zeolite. Figure 2 shows the XRD patterns of prepared zeolites with various SiO_2/Al_2O_3 molar ratio from commercial silica gel and sodium aluminate. It can be observed that the SiO_2/Al_2O_3 ratio of starting materials has significant influence on the synthesis. Only suitable SiO_2/Al_2O_3 ratio (30–40) can produce the MFI-type zeolite with highly crystallinity and the lower Al content of starting materials (SiO_2/Al_2O_3 = 50–60) have generated the zeolite product

Fig. 1 Schematic representation for the sustainable synthesis of ZSM-5

accompanied by amorphous phase (Table S1), which confirmed by the broad reflection of XRD pattern in 2θ of 20–25°. Further decreasing the Al content of starting materials ($SiO_2/Al_2O_3 = 100$) has led to the formation of tetragonal SiO_2 impurity, which is dominant in the product from Al-free synthesis system (Fig. S1). Therefore, well crystalline ZSM-5 zeolite can be formed in narrow SiO_2/Al_2O_3 ratio region and the $SiO_2/Al_2O_3 = 40$ was used in follow-up research. The SEM images of products with different SiO_2/Al_2O_3 ratio are showed in Fig. 2. It can be found that the synthesized ZSM-5 zeolite possesses uneven morphology with micrometer size. Except the hexagonal crystal main body, most samples contain some needle-like particles that might be the associated impurity (Fig. 3).

It is well known that the sodium ions not only work as charge balancing in aluminosilicate zeolites, but also play a role of templating in OSDA-free synthesis process [48, 51, 52]. So, the Na_2O/SiO_2 ratio is another important factor affecting our OSDA-free synthesis of ZSM-5. Figure 4 shows the XRD patterns of samples synthesized with different Na_2O/SiO_2 ratio.

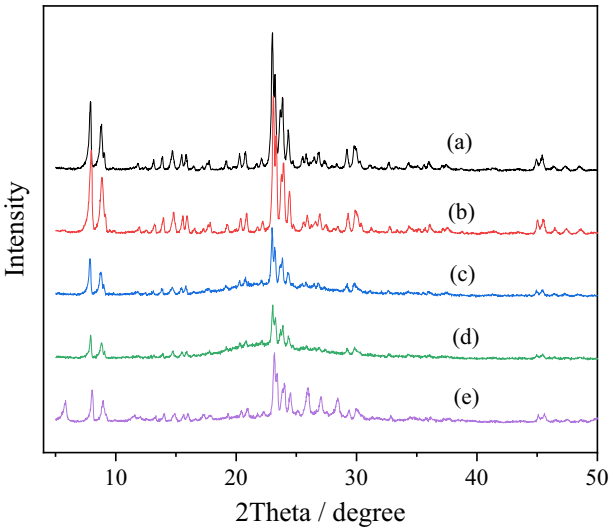

Fig. 2 XRD patterns of as-synthesized products prepared from the starting materials with SiO_2/Al_2O_3 ratio at (**a**) 30, (**b**) 40, (**c**) 50, (**d**) 60 and (**e**) 100. Synthesis condition: $Na_2O/SiO_2 = 0.072$, $H_2O/SiO_2 = 2.0$, 170 °C, 24 h

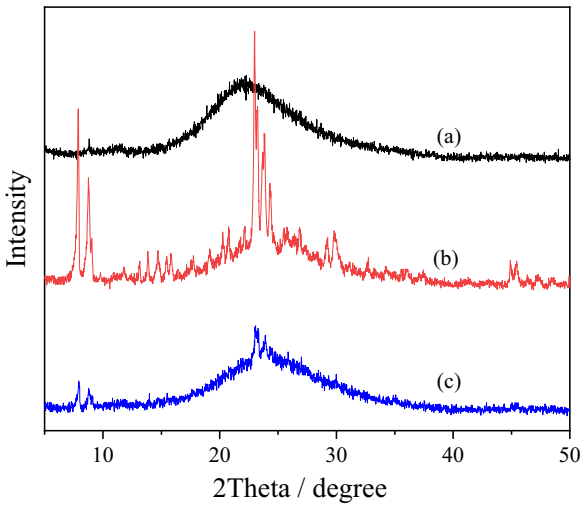

Fig. 4 XRD patterns of as-synthesized products prepared from the starting materials with Na_2O/SiO_2 ratio at (**a**) 0.036, (**b**) 0.108 and (**c**) 0.144. Synthesis condition: $SiO_2/Al_2O_3 = 40$, $H_2O/SiO_2 = 2.0$, 170 °C, 24 h

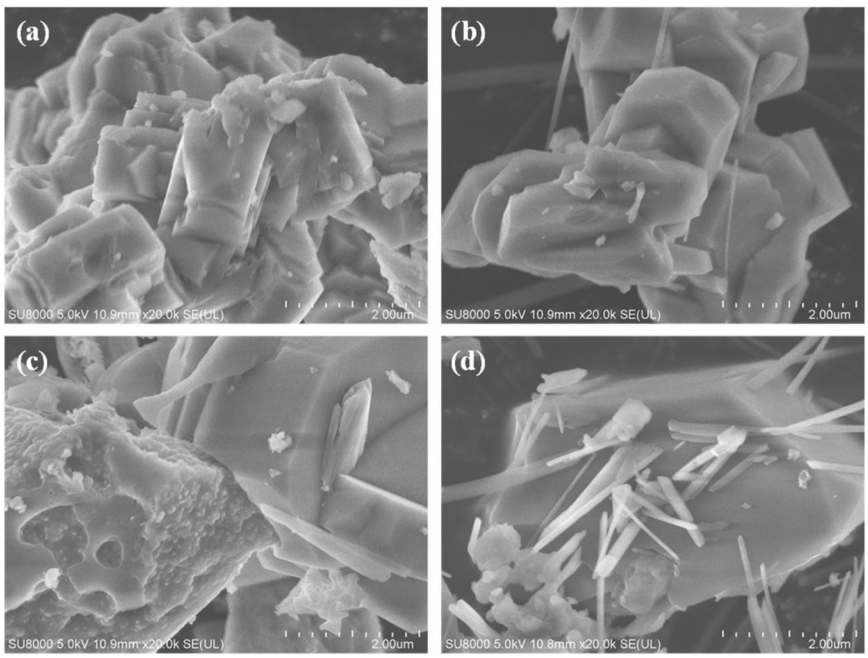

Fig. 3 SEM images of as-synthesized products prepared from the starting materials with SiO_2/Al_2O_3 ratio at (**a**) 30, (**b**) 40, (**c**) 50 and (**d**) 60. Synthesis condition: $Na_2O/SiO_2 = 0.072$, $H_2O/SiO_2 = 2.0$, 170 °C, 24 h

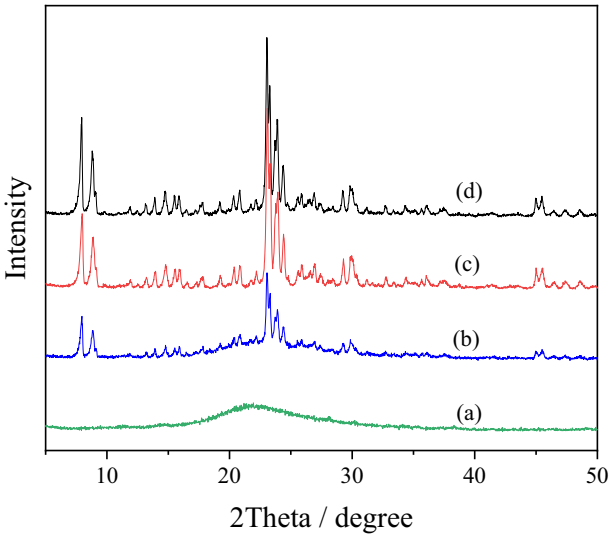

Fig. 5 XRD patterns of as-synthesized products prepared from the starting materials with H_2O/SiO_2 ratio at (**a**) 0, (**b**) 1.0, (**c**) 3.0 and (**d**) 4.0. Synthesis condition: $SiO_2/Al_2O_3 = 40$, $Na_2O/SiO_2 = 0.072$, 170 °C, 24 h

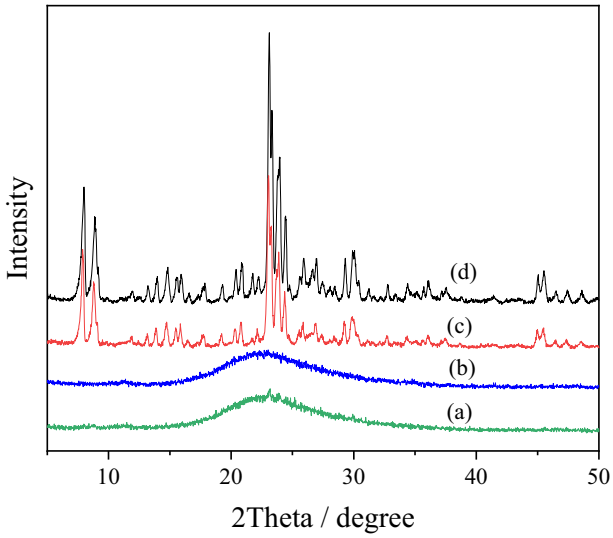

Fig. 6 XRD patterns of as-synthesized products crystalized at (**a**) 150 °C for 24 h, (**b**) 170 °C for 12 h, (**c**) 170 °C for 18 h and (**d**) 170 °C for 48 h. Synthesis condition: $SiO_2/Al_2O_3 = 40$, $Na_2O/SiO_2 = 0.072$, $H_2O/SiO_2 = 2.0$

Compared to the well crystalline product synthesized with Na_2O/SiO_2 ratio at 0.072 (Fig. 2), whether increasing or decreasing the sodium amount are unfavorable to the crystallization of product. At the Na_2O/SiO_2 ratio of 0.108, the product also exhibits well-defined MFI-type diffraction peaks with lower relative crystallinity (54%, Table S1), which will be further decreased by increasing the sodium amount. When the Na_2O/SiO_2 ratio was decreased to 0.036, no appreciable diffraction peaks can be found in the product. So, the Na_2O/SiO_2 ratio of 0.072–0.108 is suitable for this sustainable synthesis of ZSM-5. It should be noted that the sodium in our synthesis system is provided by NaOH and alumina source ($NaAlO_2$). If the NaOH is replaced by $NaHCO_3$ or the $NaAlO_2$ is replaced by aluminum sulfate while remaining the total Na_2O/SiO_2 ratio at 0.072, no MFI zeolite can be formed (Fig. S2), which may be due to the variation of the basicity of synthesis system. It follows that under premise of suitable Na_2O/SiO_2 ratio, adequate basicity is necessary to successful synthesis of MFI zeolite.

Even in the so-called solvent-free synthesis of zeolites, the water is significant and necessary. In previous reports, the crystal water of raw materials usually plays a crucial role in solvent-free synthesis of zeolites without consuming additional water, which lead to the ambiguity of the lowest level of water content for successful synthesis of zeolite [29, 48]. Herein, the employed solid silica gel contains only tiny amount of water (Fig. S3) and needs assistance of additional water with specific dosage to ensure the successful synthesis of zeolite. As a result, the dose threshold of water for successful synthesis of zeolite might be ascertained. Figure 5 indicates the effect of water amount on the synthesis of ZSM-5. As expected, MFI zeolite cannot be prepared in the water-free system. When a small amount of water was added into the synthesis system ($H_2O/SiO_2 = 1.0$), MFI crystal appeared in the product, but the relative crystallinity is lower (48%) and the amorphous phase also exists. By comparison, the H_2O/SiO_2 ratio at 2.0 generated highly crystalline ZSM-5 zeolite (Fig. 2) and the products remain well MFI structure with further increasement of water. These results confirmed the importance of water for zeolite crystallization. However, it seems that the crucial role of water is not irreplaceable. When water is replaced with an equal amount of ethanol, ZSM-5 zeolite with well crystallinity can also be synthesized (Fig. S4), which confirms the availability of organic solvent in this OSDA and solvent-free zeolite synthesis process.

Similar to the conventional hydrothermal synthesis, this sustainable synthesis process uses the common crystallization temperature at 170 °C for more than 18 h (Fig. 6). When the crystallization time is less than 12 h, or the crystallization temperature is lower (150 °C), only amorphous products can be obtained. After crystallized at 170 °C for 18 h, the product displays typical MFI structure with relative crystallinity of 61%. Further increasing the crystallization time to 24 h, the XRD of product shows the strongest peaks in intensity (Fig. 2, Table S1). When the crystallization time reaches to 48 h, the relative crystallinity of sample slightly decreased (88%). Moreover, the SEM analysis (Fig. S5) also shows that the 48h-crystallized sample contain some needle-like impurity, which cannot be found in the sample crystallized for 18 h, indicating that long crystallization time is not necessary for this sustainable synthesis for MFI zeolite. In addition, it had been reported that the pre-reactions of raw materials °Ccurred during

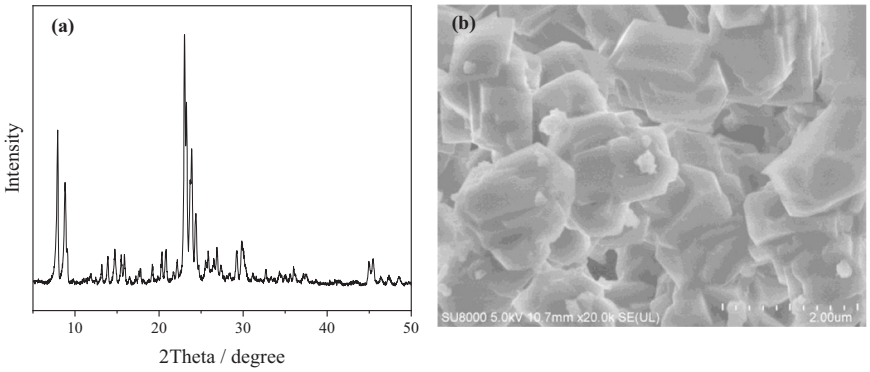

Fig. 7 XRD pattern (**a**) and SEM image (**b**) of as-synthesized samples from Stöber SiO_2 spheres. Synthesis condition: $SiO_2/Al_2O_3 = 40$, $Na_2O/SiO_2 = 0.072$, $H_2O/SiO_2 = 2.0$, 170 °C, 24 h

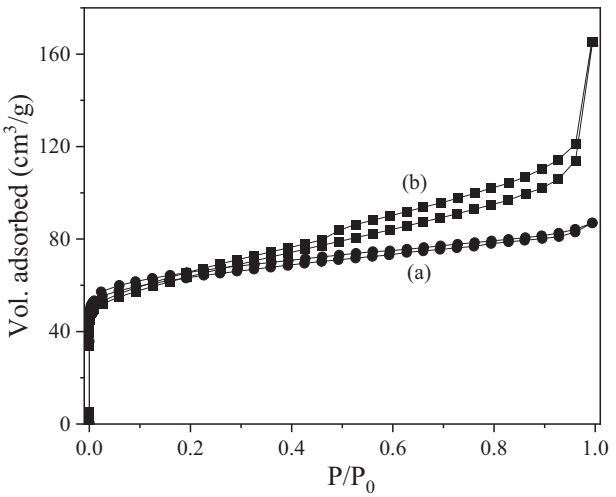

Fig. 8 N_2 physical adsorption-desorption isotherms of as-synthesized samples from (**a**) solid silica gel and (**b**) Stöber SiO_2 sphere. Synthesis condition: $SiO_2/Al_2O_3 = 40$, $Na_2O/SiO_2 = 0.072$, $H_2O/SiO_2 = 2.0$, 170 °C, 24 h

grinding are referential to the solvent-free synthesis of zeolite products [55]. In current sustainable synthesis, no identifiable crystallized products are formed in grinding stage and suitable thermal treatment is necessary to the formation of zeolite crystal, which indicates that the mechanochemical reaction in solvent-free synthesis process is associated with raw materials.

The above experiments were performed with solid silica gel as silica source. In fact, the SiO_2 spheres prepared by Stöber method are also available in this sustainable synthesis for ZSM-5. As Fig. 7 has shown, XRD pattern of the sample synthesized from Stöber SiO_2 spheres displays highly crystalline MFI structure. The SEM image exhibits irregular crystals with micrometer size regardless of the starting raw materials with uniform diameter (Fig. S6), which indicates that the Stöber SiO_2 spheres aggregate and crystallize into micro-size zeolite particles at the expense of losing original morphology. The micro scale particles and crystalline character of prepared zeolite are also confirmed by TEM and HRTEM images, respectively (Fig. S7).

Table 1 Textural properties of prepared samples

No.	Silica source	SiO_2/Al_2O_3[a] (mol/mol)	S_T[b] (m^2/g)	S_M[c] (m^2/g)	V_M[d] (cm^3/g)	V_T[e] (cm^3/g)
1	Silica gel	53	237	196	0.08	0.14
2	Stöber SiO_2	62	227	136	0.06	0.26

[a]SiO_2/Al_2O_3 molar ratio in H-type zeolites analyzed by XRF

[b]Total surface area from BET analysis

[c]Micropore surface area from t-plot analysis

[d]Micropore volume from t-plot analysis

[e]Total pore volume calculated from the adsorption at P/P_0 of 0.99

Figure 8 presents the N_2 physical adsorption-desorption isotherms of the prepared ZSM-5 zeolites and corresponding textural properties are listed in Table 1. Owing to the template-free synthesis route, the as-synthesized samples without any thermal treatment possess open porous structure. It can be found that both the zeolites from solid silica gel and Stöber SiO_2 sphere exhibit adsorption at low P/P_0 (< 0.01), confirming the presence of open micropores in the samples. Compared to the type-I isotherm of silica gel-derived sample, the zeolite from Stöber SiO_2 sphere shows a hysteresis loop at high relative pressure (0.5–0.9), which indicates that the sample contains some larger pores and leading to higher total pore volume (Table 1). In addition, the total surface areas of sustainable synthesized zeolites herein are less than that of sample from conventional hydrothermal synthesis, which may be related to the blocked effect of sodium ions and other impurities in the channel of zeolites and is in accordance with previous report [52].

The as-synthesized Na-type zeolites had been converted into H-type ones through NH_4^+- exchanging process to obtain acid properties. Figure 9 shows the NH_3-TPD profiles of the obtained H-type zeolites synthesized from solid silica gel and Stöber SiO_2 sphere. Both the samples display profiles with two intensive desorption peaks at temperature of 200–220 and 425–435 °C, indicating the weak and strong acid sites in the samples, respectively. Compared to the

zeolite from solid silica gel, the SiO_2 sphere-derived sample shows lower acid amounts, which might be associated with the difference on actual Al_2O_3 content in two samples (Table 1).

3.2 Fabrication of Pt-ZSM-5 catalysts and catalytic performance

The availability of Stöber SiO_2 spheres has expanded this sustainable synthesis route into fabrication of metal-zeolite composites, which benefit from the universality of Stöber process in constructing metal@SiO_2 hybrids [56, 57]. Herein, PVP-stabilized Pt nanoparticles from alcohol reduction process were incorporated into Stöber system, and then Pt@SiO_2 core-shell hybrid had been obtained. By utilizing this Pt@SiO_2 as silica source, the Pt@ZSM-5 composite can be synthesized through aforementioned sustainable synthesis approach. For comparison, the supported Pt/ZSM-5 was prepared via incipient-wetness impregnation with solid silica gel-derived ZSM-5 as carrier. The fabrications of Pt-zeolite catalysts are schematically described in Fig. 10.

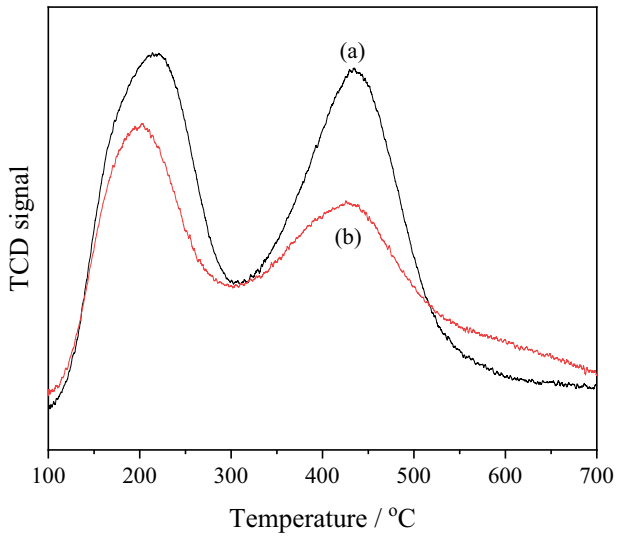

Fig. 9 NH_3-TPD profiles of H-type zeolites synthesized from (**a**) Solid silica gel and (**b**) Stöber SiO_2 sphere

The TEM analysis shows that the original Pt nanoparticles and Pt@SiO_2 hybrid possessing the metallic particles with size of 2 ~ 3 nm (Fig. 11a, b). By contrast, the prepared Pt@ZSM-5 (H-form) exhibits that slightly increased metallic nanoparticles (~5 nm) embedded in ZSM-5 matrix (Fig. 11c), which can be attributed to the thermal treatment during ion-exchange procedure. After all, serious aggregation of metal particles was avoided for the zeolite confinement effect. However, the supported Pt/ZSM-5 exhibits uneven sized metal particles with some individuals exceed 10 nm (Fig. 11d), indicating that the agglomeration of Pt nanoparticles occurred in calcination process. Even so, the XRD pattern of both Pt@ZSM-5 and Pt/ZSM-5 only displays MFI diffraction peaks with high crystallinity and no characteristic peaks associated with Pt or PtO_x phase are visible (Fig. 11e), which maybe due to the low Pt content in the samples (0.36% for Pt@ZSM-5 and 0.57% for Pt/ZSM-5). Highly crystallinity of Pt@ZSM-5 suggests that Pt nanoparticles embedded in colloid SiO_2 spheres did not hamper the formation of zeolite. When the Pt nanoparticles were directly mixed with SiO_2 spheres and other raw materials, nevertheless, a poor crystalline product had been obtained (Fig. S7). This result indicates that the OSDA and solvent-free synthesis process is susceptible to other external factors. The Pt species in the prepared catalysts were identified by XPS and is showed in Fig. 11f. Because of different synthesis approaches for the two Pt-zeolite catalysts, their Pt state is different. The XPS spectrum of Pt@ZSM-5 synthesized from Pt nanoparticles exhibits doublet signals at 71.3 eV and 74.6 eV, which are assigned to metallic Pt 4 $f_{7/2}$ and Pt 4 $f_{5/2}$, respectively [58]. The crystallization of zeolite and subsequent treatment did not change the oxidative state of Pt species. However, the Pt species in Pt/ZSM-5 prepared by impregnation method are mainly oxide (PtO). It should

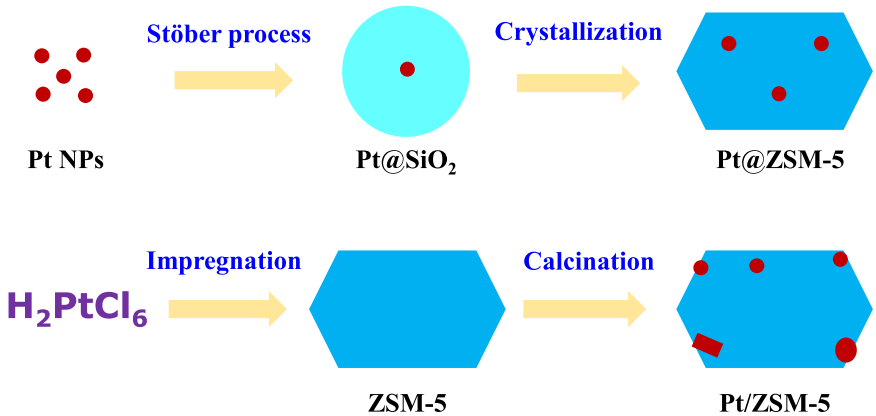

Fig. 10 Schematic representation for the synthesis of Pt-zeolite bifunctional catalysts

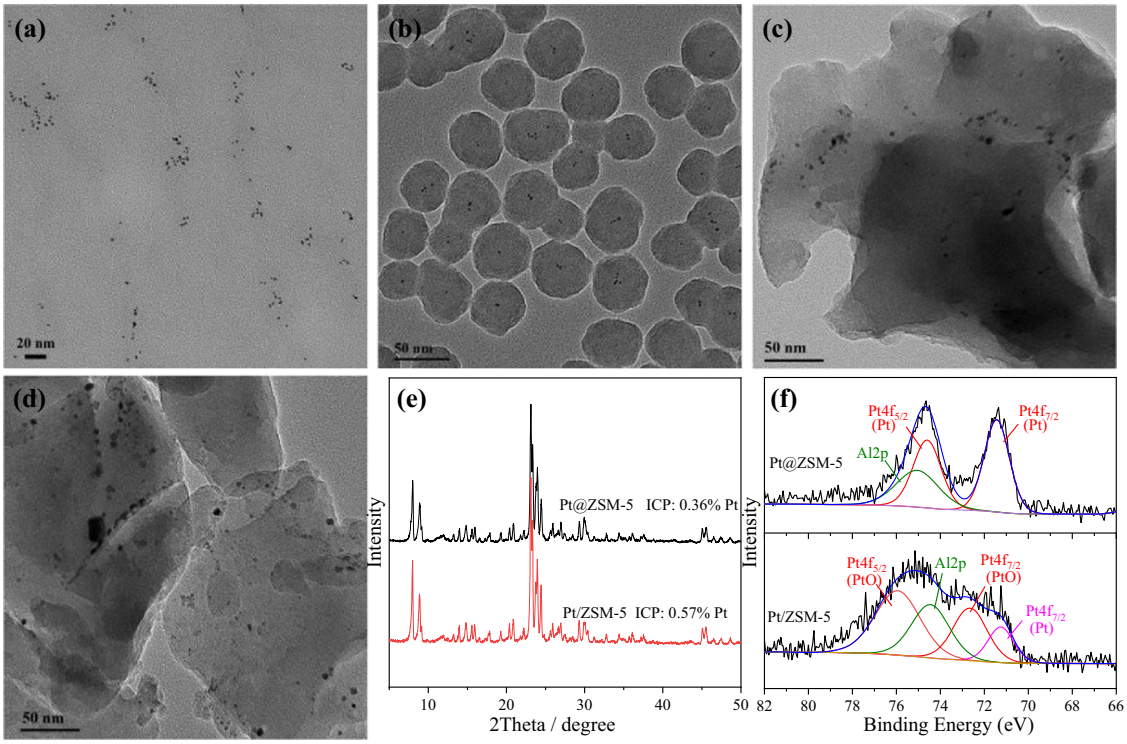

Fig. 11 TEM images of Pt nanoparticles (**a**), Pt@SiO_2 (**b**), Pt@ZSM-5 (**c**) and Pt/ZSM-5 (**d**), XRD pattern (**e**) and Pt 4f XPS (**f**) of Pt@ZSM-5 and Pt@ZSM-5

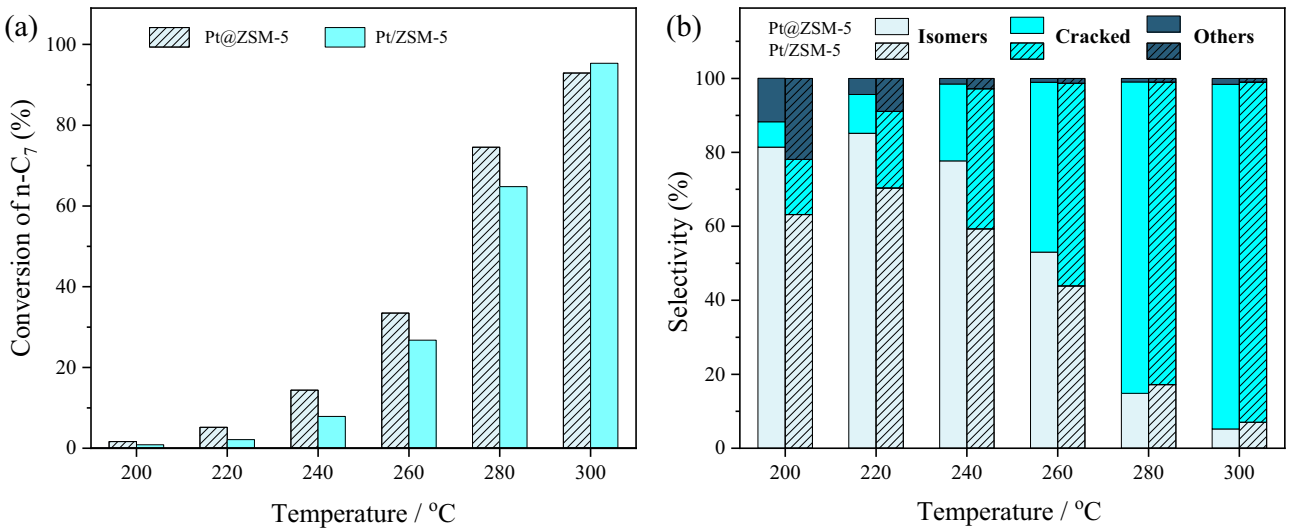

Fig. 12 Conversion (**a**) and products selectivity (**b**) of prepared Pt-ZSM-5 catalysts in hydroisomerization of *n*-heptane

be noted that the Al 2p signal is also comprised in Pt 4f XPS spectra.

The catalytic performance of prepared Pt-ZSM-5 catalysts had been investigated in hydroisomerization of *n*-heptane, which is a typical reaction catalyzed by bifunctional metal-acid catalysts [59–61]. As Fig. 12a has shown, both Pt@ZSM-5 and Pt/ZSM-5 show low *n*-heptane conversion (<5%) at lower reaction temperature (<220 °C). With the reaction temperature increasing, the *n*-heptane conversion for two catalysts also increases and is over 90% at 300 °C. However, the selectivity to isomers for both catalysts decline with the increase of temperature (Fig. 12b). For the Pt@ZSM-5, whose isomer selectivity is more than 50% when reaction temperature is below 260 °C and cracked products are predominant under higher temperature. Detailed products distribution listed in Table S2 indicate

that mono-branched 2-/3-methylhexanes and propane/isobutane dominate isomerization and cracking products, respectively, which are accordance with previous report [62]. It is generally acknowledged that acid and redox metal sites of catalysts governing the activity and product selectivity respectively for the hydroisomerization of alkane. Especially, the acid site-catalyzed isomerization reaction is considered as rate-determining step [63, 64]. Compared to the Pt/ZSM-5 catalyst, however, Pt@ZSM-5 exhibits superior *n*-heptane conversion and isomer selectivity at main investigated temperature range, regardless of its lower acid amount and Pt content. Therefore, suitable synergistic effect between acid and metal sites of bifunctional catalysts is probably more significant for hydroisomerization of alkane [65]. In addition, the different spatial organization two catalysts may be one of critical factor for different catalytic performance. The encapsulation structure of Pt@ZSM-5 may provide better metal-acid sites intimacy and excellent thermal stability [60], which is favorable to catalytic reaction. These results are instructive for preparation of highly effective bifunctional catalysts for hydroisomerization of *n*-heptane. For comparison, Pt-zeolite catalyst with conventional hydrothermal synthesized ZSM-5 nanocrystal as acid support was also prepared and tested in this reaction (Fig. S9). It can be found that the catalytic performances of both Pt@ZSM-5 and Pt/ZSM-5 are inferior to the conventional synthesized one, which may be due to the excellent accessibility of latter. Therefore, sustainable synthesis of zeolites with controllable particle size will be significant and promising.

4 Conclusion

In summary, the sustainable synthesis for ZSM-5 zeolites without organotemplates, solvents or seeds have been further developed. By using highly purity of silica sources (commercial silica gel and Stöber colloidal silica), the crucial influencing factors to the successful synthesis such as raw materials composition, crystallization temperature and time, have been obtained unambiguously. In addition, this green sustainable synthesis can also be extended to the construction of Pt-ZSM-5 bifunctional catalysts for hydroisomerization of *n*-heptane. It is revealed that the encapsulated Pt@ZSM-5 catalyst possessing excellent thermal stability and metal-acid sites intimacy, which is instructive for fabrication of effective catalysts for hydroisomerization of *n*-alkane. Despite the problems of limited Al content, relative lower surface areas and sensitive synthetic conditions, the merits on cost and environment of green synthesis determine its good prospect of application in heterogeneous catalysis.

Supplementary information The online version contains supplementary material available at https://doi.org/10.1007/s10971-024-06542-2.

Acknowledgements The authors gratefully acknowledge the financial supports from the Talent Scientific Research Fund of LNPU (2020XJJL-016).

Author contributions This manuscript was written through contributions from all authors. MZ and CJ wrote the main manuscript text. MZ and WX finished the preparation and catalytic test experiment. MZ and WL finished characterization and catalytic tests. RW and HJ participated in the discussion and analysis of experiment results. All authors reviewed the manuscript and approved the final version.

Compliance with ethical standards

Conflict of interest The authors declare no competing interests.

References

1. Li Y, Li L, Yu JH (2017) Applications of zeolites in sustainable chemistry. Chem-Us 3:928–949. https://doi.org/10.1016/j.chempr.2017.10.009
2. Corma A (1995) Inorganic solid acids and their use in acid-catalyzed hydrocarbon reactions. Chem Rev 95:559–614. https://doi.org/10.1021/cr00035a006
3. Van Speybroeck V, Hemelsoet K, Joos L, Waroquier M, Bell RG, Catlow CRA (2015) Advances in theory and their application within the field of zeolite chemistry. Chem Soc Rev 44:7044–7111. https://doi.org/10.1039/c5cs00029g
4. Moliner M, Martínez C, Corma A (2015) Multipore zeolites: synthesis and catalytic applications. Angew Chem Int Ed 54:3560–3579. https://doi.org/10.1002/anie.201406344
5. Li Y, Yu JH (2021) Emerging applications of zeolites in catalysis, separation and host-guest assembly. Nat Rev Mater 6:1156–1174. https://doi.org/10.1038/s41578-021-00347-3
6. Chi XW, Li ML, Chen X, Xu J, Yin X, Li SH, Jin ZY, Luo ZD, Wang XX, Kong DC, Han M, Xu JJ, Liu ZH, Mei DH, Wang JA, Henkelman G, Yu JH (2023) Enabling high-performance all-solid-state batteries via guest wrench in zeolite strategy. J Am Chem Soc 145:24116–24125. https://doi.org/10.1021/jacs.3c07858
7. Jiao JH, Qin YC, Zheng J, Hui Y, Zhang L, Gao XH, Song LJ (2020) Synergistic mechanism between Bronsted acid site and active cerium species in hydride transfer reaction over CeY zeolites. J Rare Earths 38:912–920. https://doi.org/10.1016/j.jre.2020.06.001
8. Li JH, Wang LN, Zhang D, Qian JH, Liu L (2020) One-step synthesis of hierarchical ZSM-5 zeolites and their catalytic performance on the conversion of methanol to aromatics. React Kinet Mech Cat 130:519–530. https://doi.org/10.1007/s11144-020-01786-9
9. Zhang HY, Cheng YT, Vispute TP, Xiao R, Huber GW (2011) Catalytic conversion of biomass-derived feedstocks into olefins and aromatics with ZSM-5: the hydrogen to carbon effective ratio. Energy Environ Sci 4:2297–2307. https://doi.org/10.1039/c1ee01230d
10. Wang DJ, Lunsford JH, Rosynek MP (1997) Characterization of a Mo/ZSM-5 catalyst for the conversion of methane to benzene. J Catal 169:347–358. https://doi.org/10.1006/jcat.1997.1712
11. Svelle S, Joensen F, Nerlov J, Olsbye U, Lillerud KP, Kolboe S, Bjorgen M (2006) Conversion of methanol into hydrocarbons over zeolite H-ZSM-5: ethene formation is mechanistically

separated from the formation of higher alkenes. J Am Chem Soc 128:14770–14771. https://doi.org/10.1021/ja065810a
12. Hammond C, Forde MM, Ab Rahim MH, Thetford A, He Q, Jenkins RL, Dimitratos N, Lopez-Sanchez JA, Dummer NF, Murphy DM, Carley AF, Taylor SH, Willock DJ, Stangland EE, Kang J, Hagen H, Kiely CJ, Hutchings GJ (2012) Direct catalytic conversion of methane to methanol in an aqueous medium by using copper-promoted Fe-ZSM-5. Angew Chem Int Ed 51:5129–5133. https://doi.org/10.1002/anie.201108706
13. Bjorgen M, Svelle S, Joensen F, Nerlov J, Kolboe S, Bonino F, Palumbo L, Bordiga S, Olsbye U (2007) Conversion of methanol to hydrocarbons over zeolite H-ZSM-5: on the origin of the olefinic species. J Catal 249:195–207. https://doi.org/10.1016/j.jcat.2007.04.006
14. Zhu ZR, Chen QL, Xie ZK, Yang WM, Kong DJ, Li C (2006) Shape-selective disproportionation of ethylbenzene to para-diethylbenzene over ZSM-5 modified by chemical liquid deposition and MgO. J Mol Catal a-Chem 248:152–158. https://doi.org/10.1016/j.molcata.2005.10.023
15. Mohammadparast F, Halladj R, Askari S (2015) The crystal size effect of nano-sized ZSM-5 in the catalytic performance of petrochemical processes: a review. Chem Eng Commun 202:542–556. https://doi.org/10.1080/00986445.2014.952815
16. Dahdah E, Estephane J, Chalouhi LM, Sammoury S, El Khoury B, Gennequin C, Abi-Aad E, Aouad S (2022) Transesterification of refined sunflower oil to biodiesel using a CaO/ZSM-5 powder catalyst. Chem Eng Technol 45:51–57. https://doi.org/10.1002/ceat.202100174
17. Singh HKG, Yusup S, Quitain AT, Abdullah B, Inayat A, Ameen M, Cheah KW, Sasaki M, Kida T, Chai YH (2021) Five-lump kinetic approach on biofuel production from refined rubber seed oil over Cu/ZSM-5 catalyst via catalytic cracking reaction. Renew Energ 171:1445–1453. https://doi.org/10.1016/j.renene.2021.02.085
18. Kadja GTM, Azhari NJ, Apriadi F, Novita TH, Safira IR, Rasrendra CB (2023) Low-temperature synthesis of three-pore system hierarchical ZSM-5 zeolite for converting palm oil to high octane green gasoline. Micropor Mesopor Mat 360:112731. https://doi.org/10.1016/j.micromeso.2023.112731
19. Al-Shafei EN, Qureshi Z, Albahar MZ, Alasseel A, Asaoka S, Aitani A (2024) Hierarchical ZSM-5@SiO_2 catalysts: a novel approach to optimizing olefin yield from heavy atmospheric gas oil. J Phys Chem C 128:10440–10449. https://doi.org/10.1021/acs.jpcc.4c03467
20. Vu HT, Lavric Z, Kostyniuk A, Drazic G, Grilc M, Likozar B, Logar NZ, Djinovic P, Tusar NN (2024) Innovative microkinetic modelling-supported structure-activity analysis of Ni/ZSM-5 during vapor-phase hydrogenation of levulinic acid. Chem Eng J 495:153456. https://doi.org/10.1016/j.cej.2024.153456
21. Russell CK, Rockey JL, Hanna RN, Miller JT (2024) Impact of Co-Fed hydrogen on high conversion propylene aromatization on H-ZSM-5 and Ga/H-ZSM-5. Catalysts 14:405. https://doi.org/10.3390/catal14070405
22. Mitra A, Cao TG, Wang HT, Wang ZB, Huang LM, Li S, Li ZJ, Yan YS (2004) Synthesis and evaluation of pure-silica-zeolite BEA as low dielectric constant material for microprocessors. Ind Eng Chem Res 43:2946–2949. https://doi.org/10.1021/ie034062k
23. Güray I, Warzywoda J, Baç N, Sacco A (1999) Synthesis of zeolite MCM-22 under rotating and static conditions. Micropor Mesopor Mat 31:241–251. https://doi.org/10.1016/s1387-1811(99)00075-x
24. Camblor MA, Corma A, Díaz-Cabañas MJ, Baerlocher C (1998) Synthesis and structural characterization of MWW type zeolite ITQ-1, the pure silica analog of MCM-22 and SSZ-25. J Phys Chem B 102:44–51. https://doi.org/10.1021/jp972319k
25. Van Grieken R, Sotelo JL, Menéndez JM, Melero JA (2000) Anomalous crystallization mechanism in the synthesis of nanocrystalline ZSM-5. Micropor Mesopor Mat 39:135–147. https://doi.org/10.1016/s1387-1811(00)00190-6
26. Song W, Justice RE, Jones CA, Grassian VH, Larsen SC (2004) Synthesis, characterization, and adsorption properties of nanocrystalline ZSM-5. Langmuir 20:8301–8306. https://doi.org/10.1021/la049516c
27. Derouane EG, Detremmerie S, Gabelica Z, Blom N (1981) Synthesis and characterization of ZSM-5 type zeolites I. physicochemical properties of precursors and intermediates. Appl Catal 1:201–224. https://doi.org/10.1016/0166-9834(81)80007-3
28. Meng XJ, Xiao FS (2014) Green routes for synthesis of zeolites. Chem Rev 114:1521–1543. https://doi.org/10.1021/cr4001513
29. Wu QM, Wang X, Qi GD, Guo Q, Pan SX, Meng XJ, Xu J, Deng F, Fan FT, Feng ZC, Li C, Maurer S, Müller U, Xiao FS (2014) Sustainable synthesis of zeolites without addition of both organotemplates and solvents. J Am Chem Soc 136:4019–4025. https://doi.org/10.1021/ja500098j
30. Liu P, Wu QM, Yan KP, Wang L, Xiao FS (2022) Solvent-free synthesis of FAU zeolite from coal fly ash. Dalton Trans 52:24–28. https://doi.org/10.1039/d2dt03196e
31. Zhou SQ, Zhou LP, Su YL, Yang XM, He H (2022) Synthesis of Sn-Beta zeolite via quasi-solid-phase route with low amount of organic template. Eur J Inorg Chem 2022:e202200130. https://doi.org/10.1002/ejic.202200130
32. Yue J, Li JJ, Liu M, Liu W, Li XJ, Xie SJ, Song CS, Guo XW, Zhu XX (2023) Amine-free synthesis of high-silica MFI zeolite by the conventional hydrothermal route. Micropor Mesopor Mat 359:112635. https://doi.org/10.1016/j.micromeso.2023.112635
33. Yin HT, Wang W, Li YX, Wen H, Chen S, Jiang NZ (2024) An eco-friendly method for the scale-up synthesis of ZSM-5 Zeolite. Micropor Mesopor Mat 365:112907. https://doi.org/10.1016/j.micromeso.2023.112907
34. Lee H, Zones SI, Davis ME (2003) A combustion-free methodology for synthesizing zeolites and zeolite-like materials. Nature 425:385–388. https://doi.org/10.1038/nature01980
35. Sang SY, Chang FX, Liu ZM, He CQ, He YL, Xu L (2004) Difference of ZSM-5 zeolites synthesized with various templates. Catal Today 93-5:729–734. https://doi.org/10.1016/j.cattod.2004.06.091
36. Feng H, Li CY, Shan HH (2009) In-situ synthesis and catalytic activity of ZSM-5 zeolite. Appl Clay Sci 42:439–445. https://doi.org/10.1016/j.clay.2008.05.004
37. Feng H, Li CY, Shan HH (2009) Effect of calcination temperature of kaolin microspheres on the in situ synthesis of ZSM-5. Catal Lett 129:71–78. https://doi.org/10.1007/s10562-008-9794-9
38. Uguina MA, Delucas A, Ruiz F, Serrano DP (1995) Synthesis of ZSM-5 from ethanol-containing systems - influence of the gel composition. Ind Eng Chem Res 34:451–456. https://doi.org/10.1021/ie00041a004
39. Ma T, Zhang LM, Song Y, Shang YS, Zhai YL, Gong YJ (2018) A comparative synthesis of ZSM-5 with ethanol or TPABr template: distinction of Bronsted/Lewis acidity ratio and its impact on n-hexane cracking. Catal Sci Technol 8:1923–1935. https://doi.org/10.1039/c7cy02418e
40. Shiralkar VP, Clearfield A (1989) Synthesis of the molecular-sieve ZSM-5 without the aid of templates. Zeolites 9:363–370. https://doi.org/10.1016/0144-2449(89)90089-4
41. Majano G, Darwiche A, Mintova S, Valtchev V (2009) Seed-induced crystallization of nanosized Na-ZSM-5 crystals. Ind Eng Chem Res 48:7084–7091. https://doi.org/10.1021/ie8017252
42. Ren N, Bronic J, Subotic B, Lv XC, Yang ZJ, Tang Y (2011) Controllable and SDA-free synthesis of sub-micrometer sized zeolite ZSM-5. Part 1: influence of alkalinity on the structural, particulate and chemical properties of the products. Micropor Mesopor Mat 139:197–206. https://doi.org/10.1016/j.micromeso.2010.10.043
43. Ren N, Bronic J, Subotic B, Song YM, Lv XC, Tang Y (2012) Controllable and SDA-free synthesis of sub-micrometer sized

zeolite ZSM-5. Part 2: influence of sodium ions and ageing of the reaction mixture on the chemical composition, crystallinity and particulate properties of the products. Micropor Mesopor Mat 147:229–241. https://doi.org/10.1016/j.micromeso.2011.06.022
44. Jablonska M, Palcic A, Lukman MF, Wach A, Bertmer M, Poppitz D, Denecke R, Wu XC, Simon U, Pöppl A, Gläser R (2023) OSDA-free seeded cu-containing ZSM-5 applied for NH_3-SCR-DeNO. Acs Omega 8:41107–41119. https://doi.org/10.1021/acsomega.3c03721
45. Wu QM, Ma Y, Wang S, Meng XJ, Xiao FS (2019) Sustainable synthesis of zeolites: from fundamental research to industrial production. Ind Eng Chem Res 58:11653–11658. https://doi.org/10.1021/acs.iecr.9b02054
46. Wu QM, Liu XL, Zhu LF, Ding LH, Gao P, Wang X, Pan SX, Bian CQ, Meng XJ, Xu J, Deng F, Maurer S, Müller U, Xiao FS (2015) Solvent-free synthesis of zeolites from anhydrous starting raw solids. J Am Chem Soc 137:1052–1055. https://doi.org/10.1021/ja5124013
47. Wu QM, Zhu LF, Chu YY, Liu XL, Zhang CS, Zhang J, Xu H, Xu J, Deng F, Feng ZC, Meng XJ, Xiao FS (2019) Sustainable synthesis of pure silica zeolites from a combined strategy of zeolite seeding and alcohol filling. Angew Chem Int Ed 58:12138–12142. https://doi.org/10.1002/anie.201906559
48. Ren LM, Wu QM, Yang CG, Zhu LF, Li CJ, Zhang PL, Zhang HY, Meng XJ, Xiao FS (2012) Solvent-free synthesis of zeolites from solid raw materials. J Am Chem Soc 134:15173–15176. https://doi.org/10.1021/ja3044954
49. Jin YY, Sun Q, Qi GD, Yang CG, Xu J, Chen F, Meng XJ, Deng F, Xiao FS (2013) Solvent-free synthesis of silicoaluminophosphate zeolites. Angew Chem Int Ed 52:9172–9175. https://doi.org/10.1002/anie.201302672
50. Pan F, Lu XC, Wang Y, Chen SW, Wang TZ, Yan Y (2014) Organic template-free synthesis of ZSM-5 zeolite from coal-series kaolinite. Mater Lett 115:5–8. https://doi.org/10.1016/j.matlet.2013.10.007
51. Chen S, Guan DD, Zhang Y, Wang Z, Jiang NZ (2019) Composition and kinetic study on template- and solvent-free synthesis of ZSM-5 using leached illite clay. Micropor Mesopor Mat 285:170–177. https://doi.org/10.1016/j.micromeso.2019.05.009
52. Liu Y, Han SY, Guan DD, Chen S, Wu YH, Yang Y, Jiang NZ (2019) Rapid green synthesis of ZSM-5 zeolite from leached illite clay. Micropor Mesopor Mat 280:324–330. https://doi.org/10.1016/j.micromeso.2019.02.027
53. Ren WG, Li J, Han LN, Wang B, Wang JC, Chang LP, Bao WR (2024) One-step synthesis of zeolite ZSM-5 from perlite tailings by crystal seed solution assisted method. Fuel 374:132489. https://doi.org/10.1016/j.fuel.2024.132489
54. Teranishi T, Hosoe M, Tanaka T, Miyake M (1999) Size control of monodispersed Pt nanoparticles and their 2D organization by electrophoretic deposition. J Phys Chem B 103:3818–3827. https://doi.org/10.1021/jp983478m
55. Nada MH, Gillan EG, Larsen SC (2019) Mechanochemical reaction pathways in solvent-free synthesis of ZSM-5. Micropor Mesopor Mat 276:23–28. https://doi.org/10.1016/j.micromeso.2018.09.009
56. Liu SH, Han MY (2010) Silica-coated metal nanoparticles. ChemAsian J 5:36–45. https://doi.org/10.1002/asia.200900228
57. Lu Y, Yin YD, Li ZY, Xia YN (2002) Synthesis and self-assembly of Au@SiO_2 coreshell colloids. Nano Letters 2:785–788. https://doi.org/10.1021/nl025598i
58. Zhou QM, Wang S, Wu ZW, Qin ZF, Dong M, Wang JG, Fan WB (2023) Aromatization of n-C_7-n-C_9 alkanes on a Pt/KZSM-5(deAl) catalyst. Catal Sci Technol 13:1009–1020. https://doi.org/10.1039/d2cy01903e
59. Noh G, Shi ZC, Zones SI, Iglesia E (2018) Isomerization and β-scission reactions of alkanes on bifunctional metal acid catalysts: consequences of confinement and diffusional constraints on reactivity and selectivity. J Catal 368:389–410. https://doi.org/10.1016/j.jcat.2018.03.033
60. Chen HM, Yi FJ, Ma CP, Gao X, Liu SY, Tao ZC, Wu BS, Xiang HW, Yang Y, Li YW (2020) Hydroisomerization of n-heptane on a new kind of bifunctional catalysts with palladium nanoparticles encapsulating inside zeolites. Fuel 268:117241. https://doi.org/10.1016/j.fuel.2020.117241
61. Oenema J, Harmel J, Vélez RP, Meijerink MJ, Eijsvogel W, Poursaeidesfahani A, Vlugt TJH, Zecevic J, De Jong KP (2020) Influence of nanoscale intimacy and zeolite micropore size on the performance of bifunctional catalysts for n-heptane hydroisomerization. Acs Catal 10:14245–14257. https://doi.org/10.1021/acscatal.0c03138
62. Kim J, Kim W, Seo Y, Kim JC, Ryoo R (2013) N-heptane hydroisomerization over Pt/MFI zeolite nanosheets: effects of zeolite crystal thickness and platinum location. J Catal 301:187–197. https://doi.org/10.1016/j.jcat.2013.02.015
63. Ma PD, Li YB, Zhou HX, Wang MH, Zhu MS, Han YY, Zhang X, Cheng K, Chowdhury AD (2023) Illuminating the impact of the proximity communication modes between redox metallic and acidic zeolite sites during hydro-conversion of n-heptane. Mater Today Chem 33:101745. https://doi.org/10.1016/j.mtchem.2023.101745
64. Cheng K, Van Der Wal LI, Yoshida H, Oenema J, Harmel J, Zhang ZR, Sunley G, Zecevic J, De Jong KP (2020) Impact of the spatial organization of bifunctional metal-zeolite catalysts on the hydroisomerization of light alkanes. Angew Chem Int Ed 59:3592–3600. https://doi.org/10.1002/anie.201915080
65. Wang W, Liu CJ, Wu W (2019) Bifunctional catalysts for the hydroisomerization of n-alkanes: the effects of metal-acid balance and textural structure. Catal Sci Technol 9:4162–4187. https://doi.org/10.1039/c9cy00499h